

## Supporting Information

# Redox-Activated Theranostic Nanoagent: Toward Multi-Mode Imaging Guided Chemo- Photothermal Therapy

Ting-Ting Zhang,<sup>†</sup> Cong-Hui Xu,<sup>†</sup> Wei Zhao, Yu Gu, Xiang-Ling Li,<sup>\*</sup> Jing-Juan Xu<sup>\*</sup> and Hong-

Yuan Chen

State Key Laboratory of Analytical Chemistry for Life Science and Collaborative Innovation  
Center of Chemistry for Life Sciences, School of Chemistry and Chemical Engineering, Nanjing  
University, Nanjing 210023, China.

<sup>†</sup> These authors contributed equally to the work.

<sup>\*</sup>Corresponding author: Tel/fax: +86-25-89687924, Email: xlli@nju.edu.cn. (X.-L. Li),  
xujj@nju.edu.cn. (J.-J. Xu)

## Experimental section

**Reagents and Materials.** Tetraethyl orthosilicate (TEOS), (3-Aminopropyl) triethoxysilane (APTES), hydrogen tetrachloroaurate (III) hydrate ( $\text{HAuCl}_4 \cdot 3\text{H}_2\text{O}$ ), 2-(N-morpholino) ethanesulfonic acid (MES), 2-ethanesulfonic acid (HEPES), sodium borohydride ( $\text{NaBH}_4$ ) and poly (vinylpyrrolidone) (PVP, MW 8000) were purchased from Sigma-Aldrich. Ethanol,  $\text{KMnO}_4$ ,  $\text{NH}_2\text{OH} \cdot \text{HCl}$  and  $\text{NH}_4\text{OH}$  were bought from Sinopharm Chemical Reagent Co., Ltd. Calcein-AM (AM), propidium iodide (PI), 2-(4-amidinophenyl)-6-indolecarbamidine dihydrochloride (DAPI), Hoechst 33342, DAPY, high glucose Dulbecco's Modified Eagle Medium (DMEM), fetal bovine serum (FBS) and cell cytotoxicity assay kit (MTT assay) were bought from Invitrogen. Hypoxyprobe<sup>TM</sup>-1 Plus Kit was purchased from Hypoxyprobe, Inc.

Aptamers (AS1411:5'- $\text{NH}_2$ -TTTTTGGTGGTGGTGGTTGTGGTGGTGGTGG-3', 5'-HS-TTTTTGGTGGTGGTGGTTGTGGTGGTGGTGG-3') were synthesized and purified by Sangon Biotech (Shanghai) Co., Ltd.

**Apparatus.** Transmission electron micrographs were obtained on JEM-1011 and JEM-2100 transmission electron microscope (JEOL Ltd., Japan). The fluorescence emission spectra were obtained on a Shimadzu fluorescence S-3 spectrophotometer (RF-5301PC, Shimadzu Co., Japan). UV-vis absorption spectra were recorded on a UV-vis spectrophotometer (Nanodrop-2000C, Nanodrop, USA). The  $\zeta$ -potential was acquired with a Malvern instrument (Nano-Z, Malvern Instruments Ltd., Britain). Confocal fluorescence images of cells were acquired with a TCS SP5 confocal microscopy (Leica, Germany). The cell viability assay was performed using a Thermo Scientific Varioskan Flash (Thermo Fisher Scientific, USA). The T1 MR images of nanomaterials before and after incubation with GSH (1 mM) were obtained on a MR scanner (ICON, Bruker BioSpin Corp.). Fluorescence images of nanomaterials before and after incubation with GSH (1 mM) were measured by fluorescence imaging system (IVIS Spectrum, PerkinElmer). Thermal images were taken by infrared thermal camera (Fotric 225-1, Fotric, China).

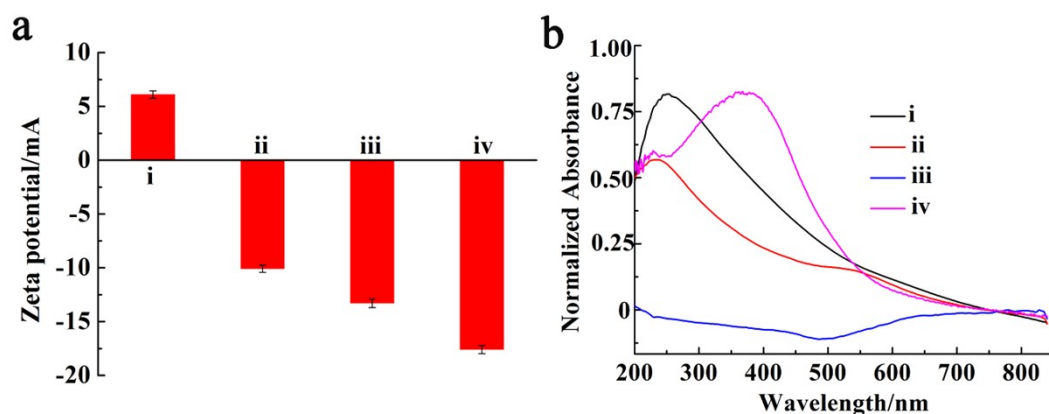


**Fig. S1** Zeta potential (a) and UV-vis-NIR absorption spectra (b) of SiO<sub>2</sub>-NH<sub>2</sub> (i), SiO<sub>2</sub>@gold seed (ii), SiO<sub>2</sub>@gold shell (iii) and SiO<sub>2</sub>@Au@MnO<sub>2</sub> (iv).

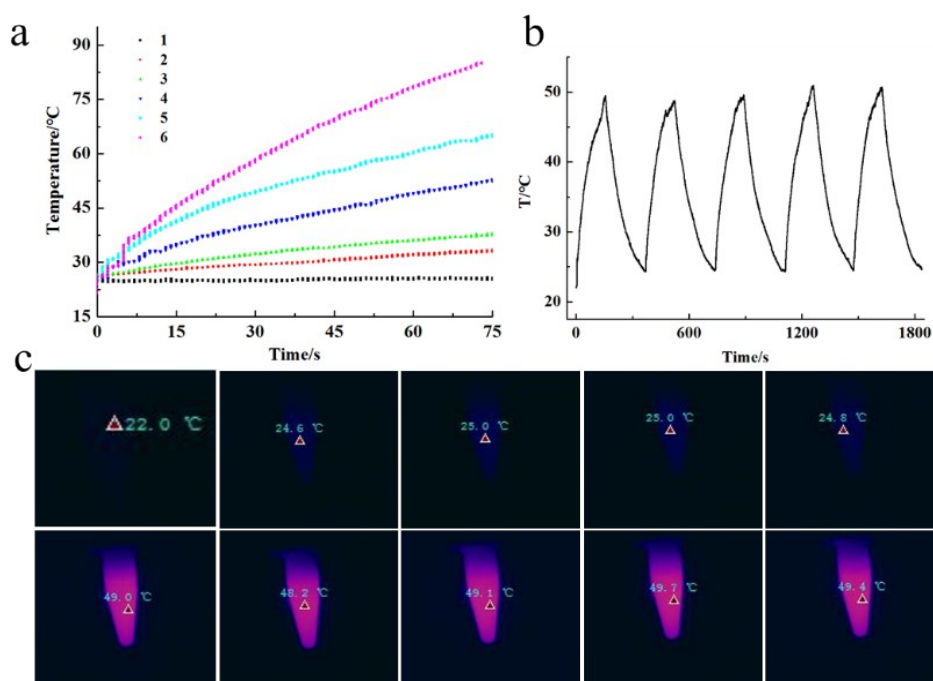


**Fig. S2** (a). Temperature change curves of the SiO<sub>2</sub>@gold shell solution with different concentrations exposed to an 808 nm laser at a power density of 2 W cm<sup>-2</sup> for 75 s, the concentrations from 1 to 6 were: 0 μg/mL, 20 μg/mL, 40 μg/mL, 60 μg/mL, 80 μg/mL, 100 μg/mL. (b). Real-time temperature measurement of SiO<sub>2</sub>@gold shell PBS dispersion under 808 nm laser irradiation with a power density of 2.0 W cm<sup>-2</sup> for 5 irradiation cycles and every cycle was composed of 2.5-min irradiation and a followed 3.5-min cooling phase. (c). Thermal imaging of the SiO<sub>2</sub>@gold shell suspension before and after NIR irradiation in each irradiation cycle.

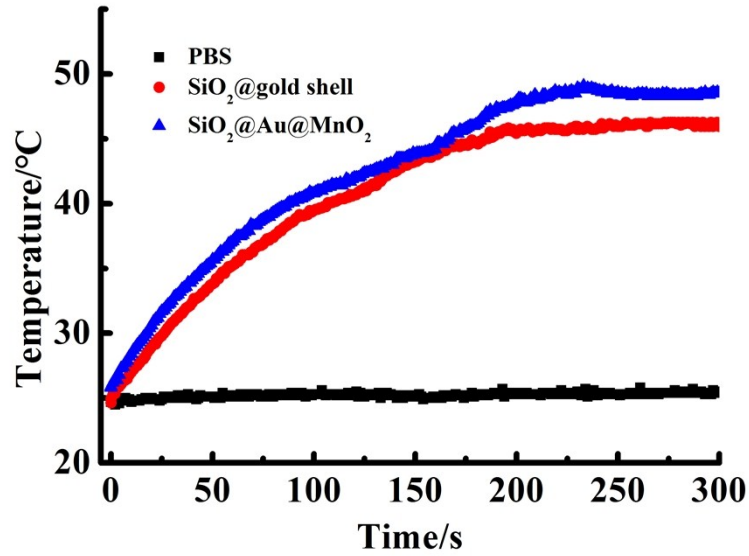


**Fig. S3** Temperature-time curves of different solutions (PBS, SiO<sub>2</sub>@gold shell and SiO<sub>2</sub>@Au@MnO<sub>2</sub>) under the irradiation of an 808 nm laser (2 W cm<sup>-2</sup>).

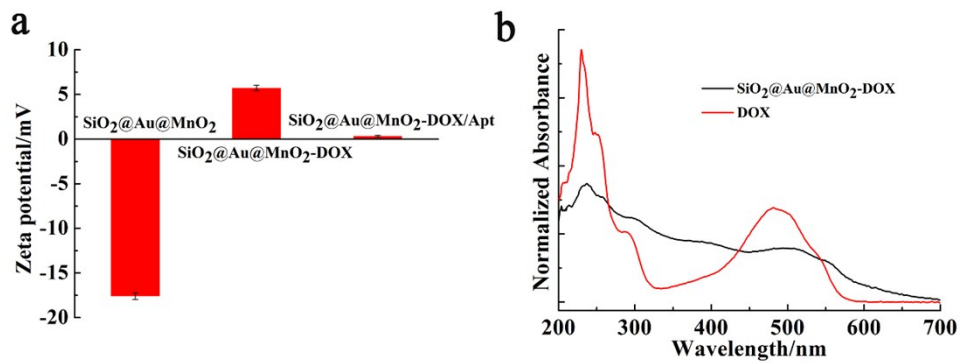


**Fig. S4** (a). Zeta potential of SiO<sub>2</sub>@Au@MnO<sub>2</sub>, SiO<sub>2</sub>@Au@MnO<sub>2</sub>-DOX and SiO<sub>2</sub>@Au@MnO<sub>2</sub>-DOX/Apt. (b). UV-vis absorption spectra of DOX and SiO<sub>2</sub>@Au@MnO<sub>2</sub>-DOX.

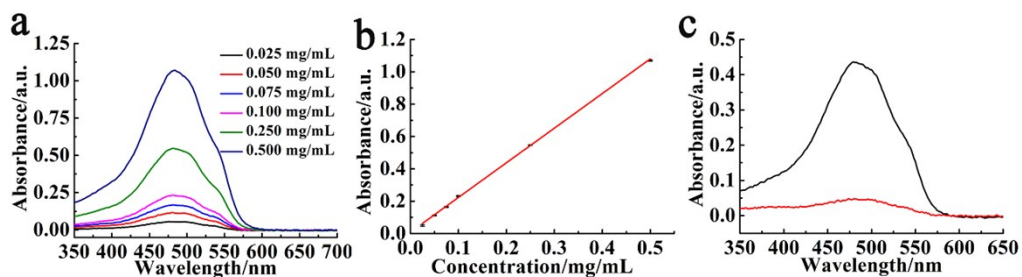


**Fig. S5** (a)-(b). The absorption intensity changes of DOX at different concentrations. (c). The absorption intensity of initial DOX and the supernatant after incubated with SiO<sub>2</sub>@Au@MnO<sub>2</sub>.

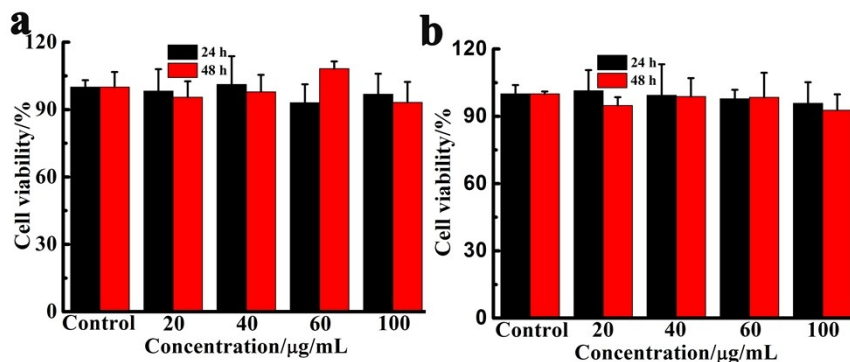


**Fig. S6** The biocompatibility evaluation of SiO<sub>2</sub>@gold shell-Apt (a) and SiO<sub>2</sub>@Au@MnO<sub>2</sub>-Apt (b). HeLa cells were incubated with different concentrations of SiO<sub>2</sub>@gold shell-Apt and SiO<sub>2</sub>@Au@MnO<sub>2</sub>-Apt for 24 h and 48 h, respectively.

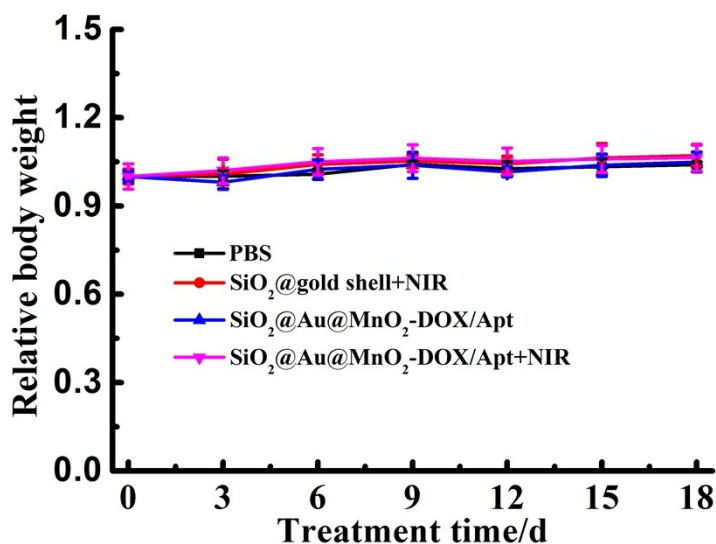


**Fig. S7** The tumor volume change curves of different groups of mice after various treatments: PBS injected (control group), group two: injected SiO<sub>2</sub>@gold shell-Apt with NIR irradiation (PTT), group three: injected SiO<sub>2</sub>@Au@MnO<sub>2</sub>-DOX/Apt (chemotherapy), group four: injected SiO<sub>2</sub>@Au@MnO<sub>2</sub>-DOX/Apt with NIR irradiation (chemotherapy/PTT).

